Research Square

Preprints are preliminary reports that have not undergone peer review.
They should not be considered conclusive, used to inform clinical practice,
or referenced by the media as validated information.

Xanthatin and 8-epi-xanthatin as new potential colchicine binding site inhibitors: a computational study

Daniel Alpízar-Pedraza
Center for Pharmaceuticals Research and Development
Ania de la Nuez Veulens
University of Havana (UH)
Yoanna María Álvarez Ginarte
University of Havana (UH)
Janet Piloto-Ferrer
Center for Pharmaceuticals Research and Development
Ángel Sánchez-Lamar (angel.sanchez@fbio.uh.cu)
University of Havana (UH)

Research Article

Keywords: docking, molecular dynamics simulations, microtubule destabilizing agents, xanthanolides, phytocompounds.

Posted Date: August 31st, 2022

DOI: https://doi.org/10.21203/rs.3.rs-1970168/v1

License: This work is licensed under a Creative Commons Attribution 4.0 International License.
Read Full License

Additional Declarations: No competing interests reported.

Version of Record: A version of this preprint was published at Journal of Molecular Modeling on January 11th, 2023. See the published version at https://doi.org/10.1007/s00894-022-05428-w.

Abstract

Phytocompounds xanthatin and 8-epi-xanthatin, obtained from *Xanthium chinese Mill,* showed antitumoral activity *in vitro,* related to the microtubules destabilizing properties of these phytocompounds. However, the exact binding pocket on tubulin of these isomers remains unknown. The aim of this work is, to develop a comprehensive computational strategy to understand and eventually predict the structure-activity relationship of xanthatin and 8-*epi*-xanthatin, with the destabilizing-antimitotic binding domain in tubulin heterodimer and to propose a putative binding site for these phytocompounds into the microtubule destabilizing agents binding sites in the tubulin heterodimer. A molecular docking was performed using the xanthanolides conformers as ligands and several tubulin structures obtained from the Protein Data Bank as receptor. The xanthanolides-tubulin complexes were energy minimized by molecular dynamics simulations at vacuum and their stability was evaluated by solvated molecular dynamics simulations during 100 ns. Xanthanolides showed higher stability into the colchicine and pironetin binding sites, whit a greater affinity for the former. In addition, the xanthanolides and non-classical colchicine binding site inhibitors share a high structural similarity.

Introduction

For decades, cancer has been the focus of many researchers. Despite all treatments available to date [1], cancer remains a very elusive disease. One of the most employed modalities to treat tumors is chemotherapy by the use of antimitotic compounds ables to disrupt the dynamic instability of microtubules (MTs) by targeting either, MTs or the MTs associated proteins (MAPs) [2].

MTs are cytoskeletal polymers of αβ tubulin that polymerize and depolymerize quickly in a nucleation mechanism. These components play an essential role in a wide number of cellular functions as the cellular division [3]. The assembly between the MTs and the kinetochores is crucial for the correct formation of the mitotic spindle and the subsequent alignment and segregation of the chromosomes [4]. Drugs that target the MTs can be classified into three main groups based on their mechanism of action: MTs-destabilizing agents (MDAs), MTs-stabilizing agents (MSAs) [5], and more recently tubulin degradation agents (TDAs) [6–8]. MDAs promote depolymerization and prevent polymerization of tubulin when it is administrated in high concentrations [9], while MSAs have an opposing effect. On the other hand, TDAs destabilize the tubulin heterodimer, promoting its unfolding, thereby inducing its degradation in a proteasome-dependent pathway [7, 8]. MDAs exert their mechanism of action over five binding sites in tubulin: colchicine binding site (CBS) [10], vinca domain [11], maytansine binding site [12], pironetin binding site [13], and the seventh site [8, 14]. MSAs interact by two well-defined pockets in the tubulin heterodimer: taxoid binding site [15] and LAU/PEL binding site [16]. Interestingly, TDAs known to date do not have distinct binding sites, they are able to bind into the colchicine domain or the seventh site [7, 8].

However, despite the wide variety of antimitotic drugs that currently exist [17, 18], these are not able to completely remove the tumor and generally promote drug resistance. It justifies the continuing work on developing and designing new candidates for antimitotic drugs. Based on their use in traditional

medicine, the plants have been widely studied for the search of new molecules with antitumoral activity [19].

The cytotoxic study of the vegetal extract from *Xanthium chinese Mill* (before known as *Xanthium strumarium)* performed by Sanchez-Lamar in 2016 [20], and Piloto-Ferrer in 2019 [21], using CHO and CT26WT cell lines, respectively, prove by the first time that the phytocompounds present in this extract could disrupt with the assembly of the mitotic spindle by MTs destabilization. The chemical fractionation allows to identify as the principal responsible of this destabilizing effect the isomers xanthatin and 8-*epi*-xanthatin [20] (Fig. 1). However, the binding pocket of these phytocompounds in the tubulin protein remains unknown. Although there are currently experimental methodologies that allow elucidating at a molecular level the mechanism of interaction of small molecules with biomolecules, these are extremely expensive and take a long time and big amounts of reagents [22]. In the last decades with the accelerated evolution in computing media and bioinformatics, theoretical procedures had emerged to help in the investigation and understanding of physical and biological phenomena of interest. The aim of this work is to propose a putative binding site for these phytocompounds into the MDAs binding sites in the tubulin heterodimer, using docking and molecular dynamics simulations.

Materials And Methods

Ligand preparation

The three-dimensional (3D) structure of xanthanolides, xanthatin and 8-*epi*-xanthatin, were obtained employing the software *ACD/Labs ChemSketch Freeware* v2018.1.1 [23]. A geometric optimization of these structures was carried out at density functional theory (DFT) level, using the hybrid functional B3LYP [24] and the base 6-31G (d,p) [25]. Optimized structures were prepared for the docking procedure employing the software AutoDock Tools v1.5.6 [26]. Final structures were saved in pdbqt file format, which is a modified protein data bank format containing atomic charges, atom type definitions, and for ligands, topological information (rotatable bonds) [27].

Receptor preparation

The 3D structures of tubulin proteins were downloaded from RSCB Protein Data Bank (PDB) (www.rscb.org) [28]. Three different structures were selected to perform the analysis in the colchicine domain, due to the T7 loop (R243-L252) adopts at least three different conformations, that can close or open the pocket, according to the assembly state and presence of an exogenous molecule in the colchicine site [29]. The PDB IDs are 3ut5 (open, the T7 loop is extended and the colchicine pocket is accessible), 5ca0 (close, the pocket is blocked by the loop), and 5c8y (middle, the loop is located in middle conformation with respect to the structures mentioned above). On other hand, for the analysis in the vinca domain and maytansine binding site only one structure of tubulin was selected (PDB ID: 3ut5). Since the pironetin binding site, is normally in a close state and is opened by Pironetin binding, a structure that contains a complex Pironetin-tubulin (PDB ID: 5fnv) was used to study this site. [13, 30]. All the PDB structures selected as receptors were first cleaned leaving only the tubulin heterodimer, the GTP, GDP, and

the Mg^{2+} ions from each subunit. Finally, the receptors were prepared for the docking using the software AutoDock Tools [26]. Because the vinca domain and the seventh site are equivalent, the results obtained for the former were assumed for both.

Docking

The complexes tubulin-xanthanolides were predicted by AutoDock Vina [31]. The conformational search space for each binding pocket was specified by a cubic box, previously defined using AutoDock Tools, each of them surrounding the destabilizing antimitotic binding pocket based on the literature evidences. The docking simulations were performed considering all rotatable angles of xanthanolides as flexible and tubulin as rigid. All parameters in the docking were established by default, with the exception of: *energy_range = 4 kcal* and *num_modes = 20.* In each of the studied binding pockets, the xanthanolides-tubulin complexes obtained were clustered using ligand root mean square deviation (RMSD) value of 2 Å [32] as criteria. From each cluster, one structure was selected as the representative binding conformation based on the lower value of the AutoDock Vina scoring function.

Optimization of xanthanolides-tubulin complexes

Xanthanolides-tubulin representative binding conformations obtained from docking were used as the start point. Xanthanolides parameters were obtained using the VMD [33] plugin FFTK (force field tool kit) [34]. On other hand, the parameters for non-protein components of receptors (GTP, GDP, Mg^{2+}) were obtained from the online server CGenFF (https://cgenff.paramchem.org) [35]. Molecular dynamics simulations were performed at vacuum, using the software NAMD v2.12 [36] and CHARMM36 force field [37]. An NVT ensemble was employed, and only the backbone of the amino acid residues around 10 Å from ligand was used as flexible, the rest was set as rigid. The temperature was fixed at 310 K and was controlled with a Langevin thermostat [38]. The timestep used was 2 fs, first, a minimization for 1ps was performance followed by 500 ps of simulation.

Stability analysis of solvated xanthanolides-tubulin complexes

The final position of optimized xanthanolides-tubulin complexes was used as the start point. The systems were solvated and the charge neutralized using Na^{+} and Cl^{-} at a final concentration of 0.05 mol/L, using the VMD plugins *Solvate* and *Autoionize* respectively. A cubic box of solvation was generated, surrounding each complex at a distance of 20 Å from the complex surface to the borderline of the box, and using the explicit solvent model TIP3 [39]. The simulations were performed using the software NAMD v2.12 [36], the CHARMM36 force field [37], and under periodic boundary conditions. An NPT ensemble was used, the temperature was fixed at 310 K and the pressure at 1 bar, these parameters were controlled using a Langeving thermostat and barostat [40] respectively. The minimization time was 1 ps and the production was for 100 ns with a timestep of 2 fs.

Binding free energy calculations using the LIE-D methodology

The binding free energy calculation of the xanthanolides-tubulin complexes that remains stable after 100 ns of the simulation was calculated using the linear interaction energy methodology improved by Miranda and coworkers in 2015 [41]. The LIE-D formula (Eq. 1) takes into account the intra-ligand electrostatic interactions as suggested by Almlöf and coworkers [42]:

$$\Delta G_{bind} = \beta(\Delta \langle V_{l-s}^{el} \rangle + \Delta \langle V_{l-l}^{el} \rangle) + \alpha \Delta \langle V_{l-s}^{vdw} \rangle + \gamma$$

(1)

Where $\Delta \langle V_{l-s}^{el} \rangle$ and $\Delta \langle V_{l-l}^{el} \rangle$ terms indicate the change in electrostatic interactions

when the ligand is transferred from the solution (free state)

into the solvated receptor binding site (bound state). $\Delta \langle V_{l-s}^{vdw} \rangle$ denotes the change in van der Waals interactions between the bound and the free state. A β value of 0.43 was calculated with the β_{FEP} specific values for each ligand using the parameterization model E proposed by Almlöf and coworkers [42] (Table 1) and Eq. 2:

$$\beta_{FEP} = \beta_0 + \frac{\sum_i w_i \Delta \beta_i}{\sum_i w_i}$$

(2)

Table 1
Optimized β Coefficients for Model E Proposed by Almlöf and coworkers [42]

β_0	**0.43**
$\Delta\beta_1(alcohols)$	-0.06
$\Delta\beta_2$ (1,2 - $amines$)	-0.04
$\Delta\beta_3$ (1 - $amides$)	-0.02
$\Delta\beta_4$ ($COOH$)	-0.03
$\Delta\beta_5$ ($anions$)	0.02
$\Delta\beta_6$ ($cations$)	0.09
$\Delta\beta_7$ ($others$)	0

where w_i, β_0, and $\Delta\beta_i$ were calculated from explicit solvent FEP calculations of single chemical groups (Table 1). This model uses w_i = 1 and w_i = 11, for all neutral and charge groups (anions and cations), respectively [42]. A value of α = 0.18 was employed, as it seems to be a robust value from previous works [43–45]. The γ coefficient value, was calculate by the Eq. (3) proposed by Miranda and coworkers, 2015 [41]:

γ = 0.95D − 2.06 (3)

where the parameter D define the balance (difference) between electrostatic (polar) and van der Waals (nonpolar) contributions to binding free energy in the LIE-method by the equation:

$D = \beta(\Delta \langle V_{l-s}^{el} \rangle + \Delta \langle V_{l-l}^{el} \rangle) - \alpha \Delta \langle V_{l-s}^{vdw} \rangle$ [kcal/mol] (4)

The $\Delta \langle V_{l-s}^{el} \rangle$, $\Delta \langle V_{l-l}^{el} \rangle$, and $\Delta \langle V_{l-s}^{vdw} \rangle$ values were calculated from the generated trajectories for each ligand-protein complexes and the xanthanolides alone in solution. The energy values were calculated using the plugin *NAMD Energy* implemented in VMD software.

Results

Xanthanolides-tubulin complexes obtained by docking

A total of 54 xanthanolides-tubulin representative conformations were obtained, 12 in the colchicine binding site (CBS), 17 in the vinca domain, 10 in the maytansine binding site, and 15 in the pironetin binding site (Supplementary table 1). Two specific orientations were observed for the xanthanolides in the colchicine and pironetin binding sites. In the xanthanolides-colchicine binding site complexes, one, present the xanthanolides γ-lactamic ring pointing toward α-subunit of the tubulin heterodimer, while in the second one, it was pointing to the β-subunit (Fig. 2A). In the pironetin binding site, one presented the γ-lactamic ring oriented to the cysteine 136 of the α-subunit (Cα136) and the aliphatic chain to the Cα4, while the other was inverted respect to the previous one (Fig. 2B). The energy range predicted by the AutoDock Vina scoring function, for the obtained complexes were around − 8.5 to -6 kcal/mol and − 8.2 to -5.5 kcal/mol, for colchicine and pironetin binding sites, respectively. Among these representative conformations, poses 5, 6, 11, and 12 in the colchicine binding site, and 40, 48 in the pironetin binding site, highlight as the most stables conformations with the lower energetic values of the 54 obtained results. Additionally, was also observed that, in the xanthanolides-colchicine binding site complexes, the energy tends to be lower as the conformation of the binding site was more closed (Supplementary table 1).

On the other hand, several representative conformations were obtained with random orientations in the vinca domain and maytansine binding site. For the study of the vinca domain, was necessary to split it on two, because according to Vinblastine binding inhibition studies [46], two different subsites have been identified in this domain: the dolastatin (Dol) [47] and vinblastine (Vlb) [48]. These subsites share a small region made up of T5 and H6-H7 loops. However, the dolastatin binding subsite reaches the helix H1

(Gβ10-Sβ25), extending the definition of the vinca domain [47]. Due to this, the docking was performed in each of the vinca domain subsites separately. The energy range predicted by the AutoDock Vina scoring function, for the obtained complexes were around − 5.8 to -4.4 kcal/mol and − 6.5 to -4.5 kcal/mol, for vinca domain (both subsites) and maytansine binding sites, respectively (Supplementary table 1). As can be observed the complexes obtained in these binding sites present higher energetic values with respect to the colchicine and pironetin binding sites. With these results was created a hierarchy order to the possible stability of the xanthanolides in each of the MDAs binding sites in tubulin been, colchicine binding site > pironetin binding site > maytansine binding site > vinca domain.

Xanthanolides-tubulin complexes optimization

The molecular docking was performed using the xanthanolides as flexible but the protein as rigid. In order to consider the flexibility of the sidechain of amino acids in the binding site, a 500 ps molecular dynamic simulation was performed at vacuum. This short simulation allows a better selection of the most relevant docking poses for further analysis. In the xanthanolides-colchicine binding site, xanthanolides showed small variations in all selected structural variants of tubulin after 500 ps of MD simulation at vacuum. At the end of the simulation was observed that, when the T7 loop is in the open conformation, the xanthanolides locate close to the αβ-tubulin interphase; however, as the loop closes the pocket, xanthanolides are deeper internalized in the domain, increasing the possibility of interacting with a higher number of amino acid residues (Supplementary Fig. 1). This fact points to a possible entry mechanism of the xanthanolides into the colchicine binding site.

At the end of the 500 ps of simulations of the xanthanolides-pironetin binding site complexes, different results were observed. Some poses show small variations from the start position, but others change their conformation and some of these even adopt similar conformations such as the poses 49 and 51, 45 and 46, 43 and 47, 40 and 44, 41 and 42 (Supplementary Fig. 2). From these were discarded for the further studies the poses 49, 46, 47, 40, and 42 according to the RMSD value obtained in the molecular dynamic simulation and the energy in the docking procedure. Additionally, both xanthanolides seems to be more stable when their γ-lactamic ring were pointing to the Cα4 than when they point to the Cα316. In the last case, xanthanolides tend to be located in the exit cleft of the domain and the RMSD values were higher (Supplementary Fig. 2).

In the vinca domain, xanthanolides converge to similar results in each of the subsites after 500 ps of MD simulation at vacuum. In both, Vlb (Supplementary Fig. 3) and Dol subsites (Supplementary Fig. 4), it is observed that even starting from different conformations in the initial time (t = 0), at the end of the simulation (t = 500 ps), all poses tended to adopt the same two representative conformations. In the first one, the xanthanolide γ-lactamic ring is directed toward the hydroxyl group (-OH) of Tyrosine 210 (Yβ210) and the aliphatic tail to the amine group (-NH) of the peptide bond of Yβ224. The second one is inverted with respect to the previous one. The first conformation showed greater representativeness than the second one for both xanthanolides in both subsites. Additionally, pose 15, which presented the highest value in the binding energy predicted by the AutoDock Vina scoring function, leave the binding site during the molecular dynamic simulation (Supplementary Fig. 4). From each of these groups were selected for

next studies the poses that show the lower RMSD value, for xanthatin: poses 18 and 19, and for 8EX: 22 and 25.

In the maytansine binding site, both xanthanolides also tend to adopt two different conformations equally represented at the end of the 500 ps of simulations. In one of these, the γ-lactamic ring is parallel to the indole ring of the Tryptophan 407 (Wβ407), while in the other, it is pointing to the hydrogen of the -NH group of the Wβ407 indole ring. Like in the vinca domain, some conformations leave the estimated sites by docking: poses 33 and 39, which also presented the highest values in the binding energy predicted by the AutoDock Vina scoring function (Supplementary Fig. 5). From each of these groups were selected for next studies the poses with the lower RMSD value, for xanthatin: poses 31 and 32, and for 8EX: 34 and 35.

Stability evaluation of the xanthanolides-tubulin complexes.

According to the obtained results by the docking procedure, the most stable complexes after 100 ns of molecular dynamic simulations were those belonging to the xanthanolides in the colchicine and pironetin binding sites. In the colchicine binding site, both xanthanolides showed minimal changes with RMSD values close or lower than 5 Å, showing a fast saturation of the curve and few fluctuations. This result suggests ligand stability in this binding site (Fig. 3A and B). However, in the pironetin binding site, even though xanthanolides remain in the domain after 100 ns, some complexes have a major structural change that can be as large as 10 Å of RMSD values. Many of these poses with high RMSD values tend to locate in the exit cleft of the domain as happened in the previous sections. Additionally, they present high fluctuations, meaning low stability of the ligand binding conformation (Fig. 3C and D).

On the other hand, the complexes evaluated for the vinca domain and the maytansine binding site showed very low stability after 100 ns of molecular dynamic simulation. RMSD values bigger than 15 Å were obtained for all complexes, which is associated with low stability and with the dissociation of the ligand from the receptor. In all cases, the xanthanolides dissociate before 20 ns of simulation (Fig. 4). These results match with the proposed hierarchical order to the possible stability of the xanthanolides in each of the MDAs binding sites of tubulin using the energies predicted by the AutoDock Vina scoring function for the obtained complex.

In order to propose the most probable MDAs binding site to the xanthanolides on the tubulin, the LIE-D methodology was used to calculate the energy of the stable ligand-receptor complexes after 100 ns of simulation. The xanthanolides-colchicine binding site complexes showed the lowest values of energy from − 6.79 to -5.21 kcal/mol (Table 2). The interaction analysis reveals that these complexes are stabilized mainly by hydrophobic interactions with amino acid residues from both subunits predominating those from zone 2 of the colchicine binding site. Furthermore, interactions with residues from all three CBS zones were observed in most of the complexes, especially when the T7 loop had intermediate and closed conformations. On the contrary, when the loop was in an open conformation, the xanthanolides were located near the interface of the heterodimer interacting only with zones 1 and 2. On the other hand, in the pironetin binding site, xanthanolides have higher values of energy than in CBS

(from − 6.94 to -3.93 kcal/mol) (Table 2), and in most cases, its tends to be located in the exit cleft of the pocket.

Table 2
Binding free energies (kcal/mol), obtained with LIE-D methodology, for each of the xanthanolides-MDAs binding sites in tubulin complexes that remain stables after 100 ns of simulation.

Colchicine Binding Site				**Pironetin Binding Site**			
Xanthatin		8-*epi*-Xanthatin		Xanthatin		8-*epi*-Xanthatin	
pose	ΔG (kcal/mol)	pose	ΔG (kcal/mol)	pose	ΔG (kcal/mol)	pose	ΔG (kcal/mol)
1	-6.79	11	-5.99	45	-6.94	48	-6.08
2	-5.91	7	-5.82	41	-4.99	52	-6.00
4	-5.57	8	-5.70	44	-4.57	50	-4.95
6	-5.46	10	-5.50	43	-3.93	53	-4.91
3	-5.44	12	-5.40			51	-4.41
5	-5.21	9	-5.36			54	-4.06

Discussion

From docking experiments, the vinca domain and maytansine binding site showed energy values higher than those observed in the colchicine and pironetin binding site. These results allow us to propose a hierarchy order to the possible stability of the xanthanolides in each of the MDAs binding sites in tubulin: colchicine binding site > pironetin binding site > maytansine binding site > vinca domain. At the end of the 100 ns of simulations, the previous results become stronger, the results obtained in the vinca domain and maytansine binding site showing high RMSD values (> 15 Å). This is related to the dissociation of the ligand from the receptor, situation corroborated visualizing the molecular dynamic trajectory with VMD. Because the vinca domain and the seventh site are equivalent, the results obtained for the former were assumed for both. However, in order to validate this hypothesis, further studies are required.

On the other hand, the result obtained in the CBS and pironetin binding site showed stability along the molecular dynamic trajectory. In the first case, the RMSD obtained, showed minimal changes in the interaction of the ligand with the receptor, obtaining always values close or lower than 5 Å and a fast saturation of the curve, suggesting ligand stability in this domain [49]. In contrast, in the pironetin binding site, some RMSD values were higher and the curve presented big fluctuations related to low stability in the interactions between the ligands and the receptor. All previous results and the energy obtained with the LIE-D methodology suggest that the xanthanolides could interact through both, the colchicine and pironetin binding site, with greater affinity for the former.

In a recently published work, was shown that the compound Cevipabulin binds indistinctly into the vinca domain and the seventh binding site, which are equivalents but located in different subunits [8]. In this sense, a superposition study based on the sequence identity homology shared by α- and β-tubulin, the 3D structures similarities, and the disposition of pironetin and colchicine binding sites in their respective subunits reveal that these are equivalent sites from different subunits. They share the same fold and their sequences are similar, with 34% of sequence identity and many of the observed amino acid changes are conservative (29%) [50]. All mentioned above, make stronger our previous suggestion of two possible binding sites in tubulin for xanthanolides.

The higher stability observed for xanthanolides in colchicine and pironetin binding sites, against the vinca domain and maytansine binding site, could be for several reasons. First, the structural characteristics of each domain, the colchicine and pironetin binding sites are well-defined deep hydrophobic pockets [18, 30, 51], while the other sites are wider and more superficial, providing few hydrophobic interactions for the stability of xanthanolides. This leads to the antimitotic drugs that bind into the colchicine and pironetin binding sites being hydrophobic low molecular weight compounds [10, 30], while those that bind at the vinca domain and maytansine binding site have more complexes structures and bigger sizes, being in many times small peptides [18, 52]. Thus, considering that xanthanolides are compounds with a hydrophobic core with few hydrogen acceptors, two at one end (O17 and O18) and one in the other (O16), and low molecular weight, they can establish more favorable interaction in a well-defined hydrophobic pocket as the colchicine and pironetin binding site.

Additionally, pharmacophoric models that can help to understand the higher selectivity of the xanthanolides for the colchicine binding site have been developed. For the colchicine binding site, two pharmacophoric models have been proposed [53, 54]. In one of them, exist seven pharmacophoric points: three hydrogen acceptors atoms (A1, A2, and A3), one hydrogen donor atom (D1), two hydrophobics centers (H1 and H2), and one planar group (R1). However, to make the molecule bioactive it only requires at least one hydrogen acceptor atom, two hydrophobic centers, and a planar group [53]. The other pharmacophore was proposed by Wang and coworkers, 2016, in which five pharmacophoric points are proposed: three hydrophobic centers (I, II, and III) and two hydrogen bond centers (IV and V, either hydrogen bond acceptor or donor). Also, they calculate the distance to which these pharmacophoric points should be found: I-II (4–9 Å), II-III (4–8 Å), III-IV (3–5 Å), V-II (4.5-7 Å), II-IV (4.5-7 Å) y IV-I (5–6 Å) [54].

For the maytansine binding site and vinca domain, pharmacophoric models have also been proposed. The first one was suggested by Prota and coworkers in 2014 for the maytansine binding site, it consists of three keys interaction points (I, II, and III) with the β-subunit of tubulin. The proposed distance between these pharmacophoric points was much higher than those raised for the colchicine binding site: I-II (10.7–12.1 Å), II-III (7.4–8.4 Å) y III-I (4.7-5 Å) [12]. The second one. was proposed by Wang and coworkers in 2015, for the vinca domain, it contains two hydrophobic groups (I and II), and three hydrogen bond forming atoms. The two hydrophobic groups I and II interact with hydrophobic pockets β and α respectively. The three-hydrogen bond forming atoms interact with Dβ179 (one N atom) and Nα329

(one N and one O atom). There are two areas (A and B) at the opposite sides of the pharmacophore where extra chemical groups can be added to make additional interactions to increase the affinity of the ligand. As for previous pharmacophores, the possible distance between the pharmacophoric points was recommended: I-II (8.5–11.2 Å), II-N (5.8-8 Å), I-N (9-10.2 Å) [52].

Xanthanolides, xanthatin and 8-epi-xanthatin, are hydrophobic molecules with a representative core constituted by a bicyclic γ-lactamic ring which contains a seven-member ring fused with a five-member ring [55]. The first ring has an aliphatic branch while the second one has a methylene group. Additionally, they contain three oxygen atoms acting as hydrogen acceptors, enabling the interaction stabilizations by hydrogen bonds. According to these structural features, we propose preliminary pharmacophore model composed by five points: three hydrophobics centers (I, II, and III) and two hydrogen acceptors (IV and V) (Fig. 5). Points I and II are represented by the methyl (C15) in the aliphatic chain and the methylene (C13) from the five-member fused ring, respectively. Point II is a bulk hydrophobic center represented by the seven-member ring. The hydrogen acceptor center is the O16 (point IV) and O18 (point V). Distance between these points was measured (I-II: 6.70 Å, II-III: 4.06 Å, III-IV: 2.96 Å, V-II: 4.99 Å, II-IV: 5.89 Å, IV-I: 2.40 Å), and show to be similar to those proposed by Wang and coworkers in the pharmacophore model for the colchicine binding site [54] (Fig. 5). In addition, these proposed pharmacophoric points in xanthanolides, are distributed in such a way that if the γ-lactamic ring is pointing toward either, α or β-subunit, these keep a similar location and distances justifying the issue that two models equally stable were obtained in this work in the colchicine binding site. On other hand, when its isomers are compared with the pharmacophore's models proposed for the vinca domain, it does not match. This analysis of the potential pharmacophoric points of the xanthanolides has great importance for the pharmaceutical industry, leading to possible chemical modifications to improve the pharmaceutical efficiency as chemotherapeutics drugs.

Regarding the higher stability observed for the xanthanolides in the colchicine binding site than in the pironetin binding site, could be associated with several facts. The colchicine and pironetin binding sites are two well-defined hydrophobic pockets that bind small molecular weight molecules. However, despite the high similarity in their 3D structure, they present some differences in their amino acid composition [50]. These differences in the primary sequence could contribute to the lower stability observed for the xanthanolides inside the pironetin binding site. Also, the CBS is located at the interface of two unseparated subunits from the same heterodimer, providing amino acid residues from both subunits for xanthanolides interaction [10]. On the other hand, the pironetin binding site is located exclusively in the α subunit reducing the number of interactions for the stabilization of xanthanolides [56]. To date, Pironetin is the only known ligand that binds into the pironetin binding site. This pocket is usually in a closed conformation, Pironetin binding opens it with some residues shifting more than 10 Å [56]. The ethyl group of Pironetin seems to play an essential role in its action, due to the biological activity decrease in Pironetin variants where this group has been removed or replaced by other groups [57–60]. All these facts represent a challenge for binding the xanthanolides into the pironetin binding site. Also, it could explain that the xanthanolides are located at the exit of the pironetin binding site at the end of molecular dynamics simulations.

So far, our results point to the idea that the isomers xanthatin and 8-epi-xanthatin are more likely to exert their mechanism of action as MTs destabilizing agents by interacting with the colchicine binding site. Based on the analysis of Pérez-Pérez et al. [61], the colchicine domain ligands were classified into classical and non-classical colchicine binding site inhibitors (CBSIs) according to their spatial orientations. The superposition of these ligands with x-ray crystal structures indicated that classical CBSIs with more globular or butterfly-like shapes occupy zones 1 and 2, mimicking the colchicine binding mode. However, non-classical CBSIs with more planar structures tend to locate deeper into the β-subunit making use of zones 2 and 3 [18, 61]. The studied xanthanolides in this work share some structural similarities with several non-classical CBSIs leading to the idea that these isomers could exert their activity by zones 2 and 3 of the colchicine binding site. However, the interaction pattern obtained in most complexes with high stability showed interactions with amino acid residues from the three zones. To date, only two CBSIs can interact with the 3 zones, ABT- 751 [29] and 2-(6-Ethoxy-3-(3-ethoxyphenylamino)-1-methyl-1,4- dihydroindeno[1,2-c]pyrazol-7-yloxy)acetamide [62], which interact mainly with zones 1 and 2 but also establish a single hydrogen bond with the Tyrβ202 from zone 3. Nevertheless, a convergent binding pose for xanthanolides in the CBS was not obtained. Despite all point to the possibility that these isomers could be classified as novel non-classical CBSIs, further studies are required to propose an accurate binding conformation and classification for xanthanolides as CBSI.

Despite Colchicine being a cheap chemotherapeutic option, its clinical applications are limited by its toxicity. It strongly binds to tubulin in non-cancerous cells and causes impaired protein assembly, mitotic arrest, and multiorgan dysfunction [10]. Because of this, the search for new and more efficient CBS inhibitors continues to be an attractive open research field. In a previous study, it was observed that mice treated with the chemical fraction containing the xanthanolides did not show signs of toxicity, but a significant inhibitory effect in the proliferation of the tumor [21]. These results could be related to the fact that xanthanolides have lower binding energy (-6.79 A -5.21 kcal / mol) than Colchicine (-10 A -9 kcal / mol) [63] in the CBS. Xanthanolides could efficiently bind to tubulin in the cancer cells with an overexpression of these proteins associated with their exacerbated cell growth. It would increase the arrest of tumor cells in the G2 / M phase, which led to the apoptosis of these cells and the reduction of the tumor. However, in non-cancerous cells in a quiescent state, the union of the xanthanolides to tubulin will be lower, decreasing toxicity in patients.

In summary, xanthatin and 8-*epi*-xanthatin isomers could bind indistinctly into the pironetin and colchicine binding sites. However, based on our results and the features of the Pironetin binding into the pironetin binding site, these isomers seem to have a greater affinity for the CBS. Additionally, the molecular structure of xanthanolides matches with the pharmacophore model proposed for the colchicine binding domain, especially with the model suggested by Wang and coworkers in 2016. The studied xanthanolides in this work share some structural similarities with several non-classical CBSIs, which consist in a planar structure and tend to locate deeper into the β-subunit making use of zones 2 and 3 in the colchicine-binding domain.

Abbreviations

MTs: microtubules; MDAs: microtubules destabilizing agents; MSAs: microtubules stabilizing agents; TDAs: tubulin degradation agents; RMSD: root mean square deviation; CBS: colchicine binding site; CBSI: colchicine binding site inhibitors

Declarations

Acknowledgments

The author thankfully acknowledges the computer resources and the technical support provided by “Empresa de Tecnologías de la Información ETI-BioCubaFarma”.

Powered@NLHPC: This research was partially supported by the supercomputing infrastructure of the NLHPC (ECM-02).

Funding

The research that gives rise to the results presented in this publication received funds from the Office of Management of International Funds and Projects of the Ministry of Science, Technology, and Environment of the Republic of Cuba, under the code PN223LH010-030.

Declaration of Competing Interest

For institutional reasons is interesting of the authors that both, Professor Angel Sánchez Lamar and Dr. Janet Piloto Ferrer appear as corresponding authors.

Authors' contributions

All authors contributed to the study conception and design. Material preparation, data collection and analysis were performed by Daniel Alpízar-Pedraza and Ania de la Nuez Veulens. The first draft of the manuscript was written by Daniel Alpízar Pedraza and all authors commented on previous versions of the manuscript. All authors read and approved the final manuscript.

References

1. Jeyamogan S, Khan NA, Siddiqui R (2021) Application and Importance of Theranostics in the Diagnosis and Treatment of Cancer. Arch Med Res 52:131–142. https://doi.org/10.1016/j.arcmed.2020.10.016
2. Paier C, Maranhão S, Carneiro T, et al (2018) Natural products as new antimitotic compounds for anticancer drug development. Clinics 73:e813s. https://doi.org/10.6061/clinics/2018/e813s

3. Harrison M, D Holen K, Liu G (2009) Beyond taxanes: a review of novel agents that target mitotic tubulin and microtubules, kinases, and kinesins. Clin Adv Hematol Oncol 7:54–64
4. Muroyama A, Lechler T (2017) Microtubule organization, dynamics and functions in differentiated cells. Development 144:3012–3021. https://doi.org/10.1242/dev.153171
5. Kavallaris M (2010) Microtubules and resistance to tubulin binding agents. Nat Rev Cancer 10:194–204
6. Yang J, Li Y, Yan W, et al (2019) Covalent modification of Cys-239 in β-tubulin by small molecules as a strategy to promote tubulin heterodimer degradation. J Biol Chem 294:8161–8170. https://doi.org/10.1074/jbc.RA118.006325
7. Li Y, Liu Y, Zhu Z, et al (2022) Structure-Based Design and Synthesis of N-Substituted 3-Amino-β-Carboline Derivatives as Potent αβ-Tubulin Degradation Agents. J Med Chem 65:2675–2693. https://doi.org/10.1021/acs.jmedchem.1c02159
8. Yang J, Yu Y, Li Y, et al (2021) Cevipabulin-tubulin complex reveals a novel agent binding site on α-tubulin with tubulin degradation effect. Sci Adv 7:. https://doi.org/10.1126/sciadv.abg4168
9. Karen E. Gascoigne, Stephen S. Taylor (2009) How do anti-mitotic drugs kill cancer cells? Journal of Cell Science 122:2579–2585
10. McLoughlin EC, O'Boyle NM (2020) Colchicine-Binding Site Inhibitors from Chemistry to Clinic: A Review. Pharmaceuticals 13:8. https://doi.org/doi:10.3390/ph13010008
11. Dumontet C, Jordan MA (2010) Microtubule-binding agents: a dynamic field of cancer therapeutics. Nat Rev Drug Discov 9:790–803
12. Prota AE, Bargsten K, Diaz JF, et al (2014) A new tubulin-binding site and pharmacophore for microtubule-destabilizing anticancer drugs. PNAS 11:13817–13821
13. Yang J, Wang Y, Wang T, et al (2016) Pironetin reacts covalently with cysteine-316 of α-tubulin to destabilize microtubule. Nat Commun 7:12103
14. Matthew S, Chen Q-Y, Ratnayake R, et al (2021) Gatorbulin-1, a distinct cyclodepsipeptide chemotype, targets a seventh tubulin pharmacological site. Proc Natl Acad Sci 118:e2021847118. https://doi.org/10.1073/pnas.2021847118
15. Nogales E, Wolf S, A. Khan I, et al (1995) Structure of tubulin at 6.5 A and location of the taxol-binding site. Nature 375:424–7. https://doi.org/10.1038/375424a0
16. Reem Hanna, David R. Maass, Paul H. Atkinson, et al (2014) Characterizing the laulimalide–peloruside binding site using site-directed mutagenesis of TUB2 in S. cerevisiae. Mol BioSyst 10:110
17. Steinmetz MO, Prota AE (2018) Microtubule-Targeting Agents: Strategies To Hijack the Cytoskeleton. Trends Cell Biol 28:776–792. https://doi.org/10.1016/j.tcb.2018.05.001
18. Li W, Sun H, Xu S, et al (2017) Tubulin inhibitors targeting the colchicine binding site: a perspective of privileged structures. Future Med Chem 9:1765–1794. https://doi.org/10.4155/fmc-2017-0100
19. Zhang D, Kanakkanthara A (2020) Beyond the Paclitaxel and Vinca Alkaloids: Next Generation of Plant-Derived Microtubule-Targeting Agents with Potential Anticancer Activity. Cancers 12:1721.

https://doi.org/10.3390/cancers12071721

20. Sánchez-Lamar A, Piloto-Ferrer J, Fiore M, et al (2016) Xanthium strumarium extract inhibits mammalian cell proliferation through mitotic spindle disruption mediated by xanthatin. J Ethnopharmacol 194:781–788. https://doi.org/10.1016/j.jep.2016.11.006
21. Janet Piloto-Ferrer, Ángel Sánchez-Lamar, Marbelis Francisco, et al (2019) Xanthium strumarium´s xanthatins induces mitotic arrest and apoptosis in CT26WT colon carcinoma cells. Phytomedicine 57:236–244
22. S. Madhukar N, K. Khade P, Huang L, et al (2019) A Bayesian machine learning approach for drug target identification using diverse data types. NATURE COMMUNICATIONS 10:. https://doi.org/doi.org/10.1038/s41467-019-12928-6
23. (2019) ACD/Labs ChemSketch. Advanced Chemistry Development, Inc., Toronto, ON, Canada
24. Zhao Y, Truhlar DG (2008) Density Functionals with Broad Applicability in Chemistry. Acc Chem Res 41:157–167. https://doi.org/10.1021/ar700111a
25. Pople JA (1970) Molecular orbital methods in organic chemistry. Acc Chem Res 3:217–223. https://doi.org/10.1021/ar50031a002
26. Morris GM, Huey R, Lindstrom W, et al (2009) AutoDock4 and AutoDockTools4: Automated docking with selective receptor flexibility. J Comput Chem 30:2785–2791. https://doi.org/10.1002/jcc.21256
27. Seeliger D, de Groot BL (2010) Ligand docking and binding site analysis with PyMOL and Autodock/Vina. J Comput Aided Mol Des 24:417–422. https://doi.org/10.1007/s10822-010-9352-6
28. Berman HM, Battistuz T, Bhat TN, et al (2002) The Protein Data Bank. Acta Crystallogr D Biol Crystallogr 58:899–907. https://doi.org/10.1107/S0907444902003451
29. Dorléans A, Gigant B, Ravelli RBG, et al (2009) Variations in the colchicine-binding domain provide insight into the structural switch of tubulin. PNAS 106:13775. https://doi.org/10.1073/pnas.0904223106
30. Prota AE, Setter J, Waight AB, et al (2016) Pironetin binds covalently to αCys316 and perturbs a major loop and helix of α-tubulin to inhibit microtubule formation. J Mol Biol 428:2981–2988
31. Trott O, Olson AJ (2009) AutoDock Vina: Improving the speed and accuracy of docking with a new scoring function, efficient optimization, and multithreading. J Comput Chem NA-NA. https://doi.org/10.1002/jcc.21334
32. Kang L (2019) Refined Molecular Docking with Multi-objective Optimization Method. In: Xiong N, Xiao Z, Tong Z, et al (eds) Advances in Computational Science and Computing. Springer International Publishing, Cham, pp 56–63
33. Humphrey W, Dalke A, Schulten K (1996) VMD: Visual molecular dynamics. J Mol Graph 14:33–38. https://doi.org/10.1016/0263-7855(96)00018-5
34. Mayne CG, Saam J, Schulten K, et al (2013) Rapid parameterization of small molecules using the force field toolkit. J Comput Chem 34:2757–2770. https://doi.org/10.1002/jcc.23422

35. Vanommeslaeghe K, Hatcher E, Acharya C, et al (2010) CHARMM general force field: A force field for drug-like molecules compatible with the CHARMM all-atom additive biological force fields. J Comput Chem 31:671–690. https://doi.org/10.1002/jcc.21367
36. Phillips JC, Braun R, Wang W, et al (2005) Scalable molecular dynamics with NAMD. J Comput Chem 26:1781–1802. https://doi.org/10.1002/jcc.20289
37. Best RB, Zhu X, Shim J, et al (2012) Optimization of the Additive CHARMM All-Atom Protein Force Field Targeting Improved Sampling of the Backbone ϕ, ψ and Side-Chain χ_1 and χ_2 Dihedral Angles. J Chem Theory Comput 8:3257–3273. https://doi.org/10.1021/ct300400x
38. Davidchack RL, Handel R, Tretyakov MV (2009) Langevin thermostat for rigid body dynamics. J Chem Phys 130:234101. https://doi.org/10.1063/1.3149788
39. Jorgensen WL, Chandrasekhar J, Madura J, Klein M (1983) Comparison of Simple Potential Functions for Simulating Liquid Water. J Chem Phys 79:
40. Feller SE, Zhang Y, Pastor RW, Brooks BR (1995) Constant pressure molecular dynamics simulation: The Langevin piston method. J Chem Phys 103:4613–4621. https://doi.org/10.1063/1.470648
41. Miranda WE, Noskov SYu, Valiente PA (2015) Improving the LIE Method for Binding Free Energy Calculations of Protein–Ligand Complexes. J Chem Inf Model 55:1867–1877. https://doi.org/10.1021/acs.jcim.5b00012
42. Almlöf M, Carlsson J, Åqvist J (2007) Improving the Accuracy of the Linear Interaction Energy Method for Solvation Free Energies. J Chem Theory Comput 3:2162–2175. https://doi.org/10.1021/ct700106b
43. Hansson T, Marelius J, Aqvist J (1998) Ligand binding affinity prediction by linear interaction energy methods. J Comput Aided Mol Des 12:27–35. https://doi.org/10.1023/a:1007930623000
44. Marelius J, Hansson T, Åqvist J (1998) Calculation of ligand binding free energies from molecular dynamics simulations. Int J Quantum Chem 69:77–88. https://doi.org/10.1002/(SICI)1097-461X(1998)69:1<77::AID-QUA10>3.0.CO;2-2
45. Valdés-Tresanco MS, Valdés-Tresanco ME, Rubio-Carrasquilla M, et al (2021) Tailored Parameterization of the LIE Method for Calculating the Binding Free Energy of Vps34-Inhibitor Complexes. ACS Omega 6:29525–29536. https://doi.org/10.1021/acsomega.1c03582
46. Gupta S, Bhattacharyya B (2003) Antimicrotubular drugs binding to vinca domain of tubulin. Molecular and Cellular Biochemistry 253:41–47. https://doi.org/10.1023/A:1026045100219
47. Cormier A, Marchand M, Ravelli RBG, et al (2008) Structural insight into the inhibition of tubulin by vinca domain peptide ligands. EMBO reports 9:1101–1106
48. Gigant B, Wang C, Ravelli RBG, et al (2005) Structural basis for the regulation of tubulin by vinblastine. Nature 435:519–522. https://doi.org/10.1038/nature03566
49. Lone MY, Athar M, Manhas A, et al (2017) In Silico Exploration of Vinca Domain Tubulin Inhibitors: A Combination of 3D-QSAR-Based Pharmacophore Modeling, Docking and Molecular Dynamics Simulations. ChemistrySelect 2:10848–10853. https://doi.org/10.1002/slct.201701971

50. Alpízar-Pedraza D, Veulens A de la N, Araujo EC, et al (2022) Microtubules destabilizing agents binding sites in tubulin. J Mol Struct 1259:132723. https://doi.org/10.1016/j.molstruc.2022.132723
51. Tripathi S, Srivastava G, Singh A, et al (2018) Insight into microtubule destabilization mechanism of 3,4,5-trimethoxyphenyl indanone derivatives using molecular dynamics simulation and conformational modes analysis. J Comput Aided Mol Des 32:559–572. https://doi.org/10.1007/s10822-018-0109-y
52. Wang Y, Benz FW, Wu Y, et al (2016) Structural Insights into the Pharmacophore of Vinca Domain Inhibitors of Microtubules. Mol Pharmacol 89:233–242. https://doi.org/10.1124/mol.115.100149
53. Nguyen TL, McGrath C, Hermone AR, et al (2005) A Common Pharmacophore for a Diverse Set of Colchicine Site Inhibitors Using a Structure-Based Approach. J Med Chem 48:6107–6116
54. Wang Y, Zhang H, Gigant B, et al (2016) Structures of a diverse set of colchicine binding site inhibitors in complex with tubulin provide a rationale for drug discovery. FEBS J 283:102–111. https://doi.org/10.1111/febs.13555
55. Feng J, Lei X, Bao R, et al (2017) Enantioselective and Collective Total Syntheses of Xanthanolides. Angew Chem Int Ed 56:16323–16327. https://doi.org/10.1002/anie.201710846
56. Coulup SK, Georg GI (2019) Revisiting microtubule targeting agents: α-Tubulin and the pironetin binding site as unexplored targets for cancer therapeutics. Bioorg Med Chem Lett 29:1865–1873. https://doi.org/10.1016/j.bmcl.2019.05.042
57. Panos J, Diaz-Oltra S, Sanchez-Peris M, et al (2013) Synthesis and biological evaluation of truncated alpha-tubulin-binding pironetin analogues lacking alkyl pendants in the side chain or the dihydropyrone ring. Org Biomol Chem 11:5809–26
58. Marco JA, Garcia-Pla J, Carda M, et al (2011) Design and synthesis of pironetin analogues with simplified structure and study of their interactions with microtubules. Eur J Med Chem 46:1630–7
59. Roldán S, Cardona A, Conesa L, et al (2017) Synthesis and biological evaluation of simplified pironetin analogues with modifications in the side chain and the lactone ring. Org Biomol Chem 15:220–232. https://doi.org/10.1039/C6OB01585A
60. Georg G, Huang D, Wong H (2017) Synthesis and Cytotoxicity Evaluation of C4- and C5- Modified Analogues of the a,b-Unsaturated Lactone of Pironetin. ChemMedChem 12:. https://doi.org/10.1002/cmdc.201700084
61. Pérez-Pérez M-J, Priego E-M, Bueno O, et al (2016) Blocking Blood Flow to Solid Tumors by Destabilizing Tubulin: An Approach to Targeting Tumor Growth. J Med Chem 59:8685–8711. https://doi.org/10.1021/acs.jmedchem.6b00463
62. Liu Y-N, Wang J-J, Ji Y-T, et al (2016) Design, Synthesis, and Biological Evaluation of 1-Methyl-1,4-dihydroindeno[1,2-c]pyrazole Analogues as Potential Anticancer Agents Targeting Tubulin Colchicine Binding Site. J Med Chem 59:5341–5355. https://doi.org/10.1021/acs.jmedchem.6b00071
63. Chakrabarti G, Sengupta S, Bhattacharyya B (1996) Thermodynamics of Colchicinoid-Tubulin Interactions. J Biol Chem 271:2897–2901. https://doi.org/10.1074/jbc.271.6.2897

Figures

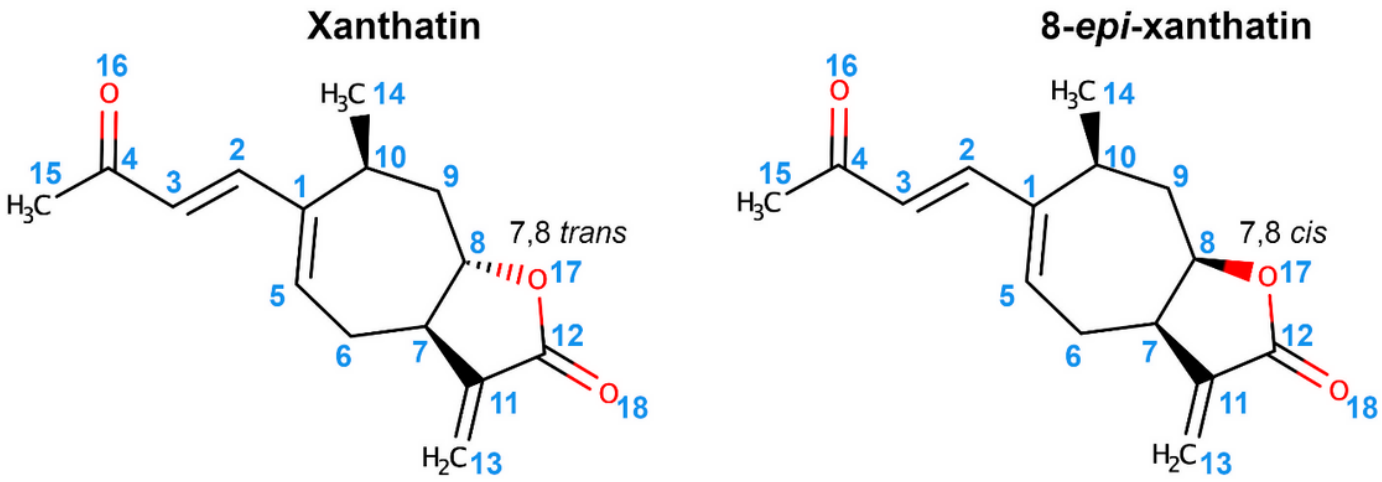


Figure 1

2D Structure of Xanthatin (left) and 8-epi-xanthatin (rigth)

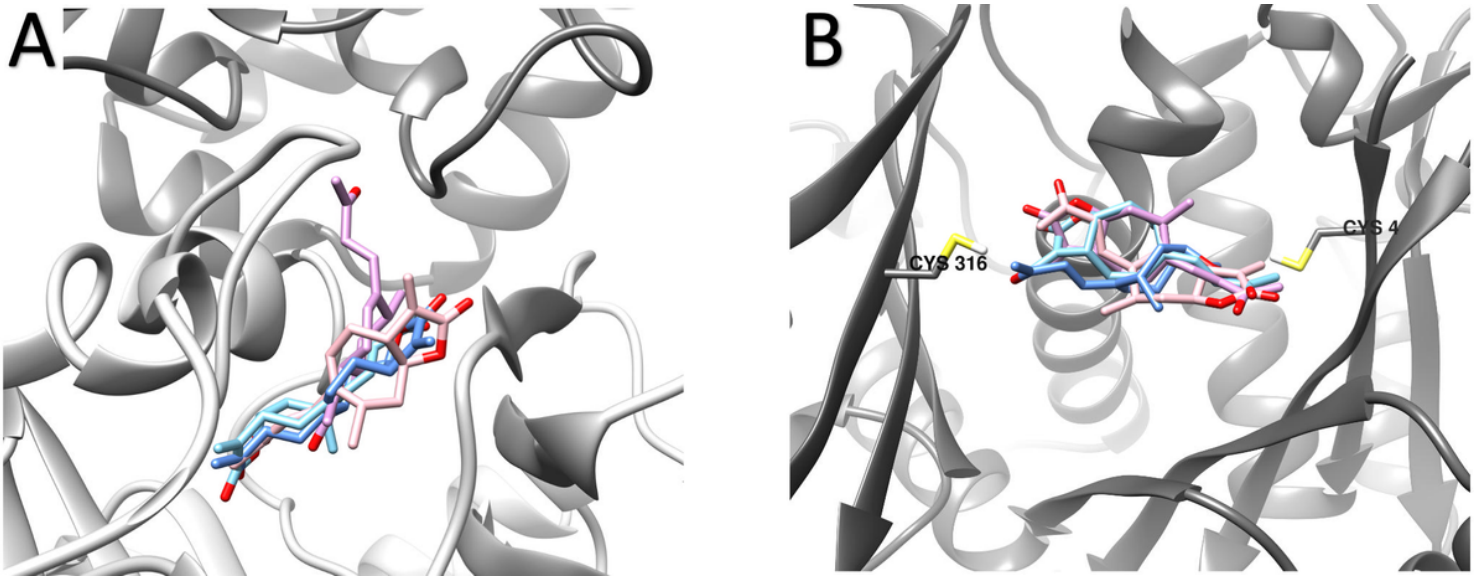


Figure 2

Representative conformation obtained for xanthatin (pink) and 8-epi-xanthatin (blue) in the colchicine binding site (A) and the pironetin binding site (B). The a- and b-subunit of tubulin are represented in dark gray and light gray ribbons, respectively

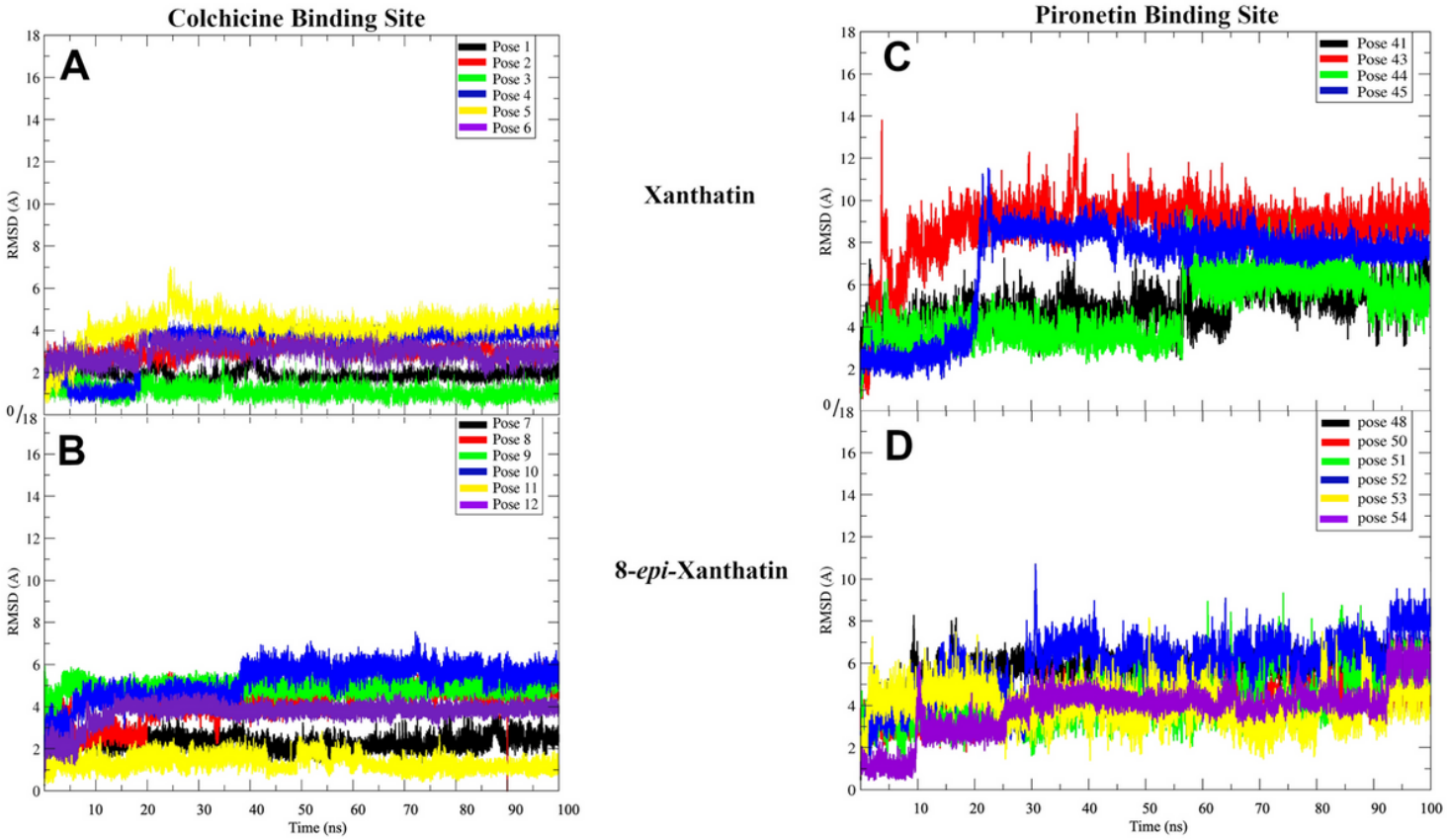


Figure 3

Root means square deviations (RMSD) corresponding to xanthanolides-colchicine and -pironetin binding sites complexes. A) xanthatin-CBS, B) 8-epi-xanthatin-CBS, C) xanthatin-pironetin binding site, D) 8-epi-xanthatin-pironetin binding site

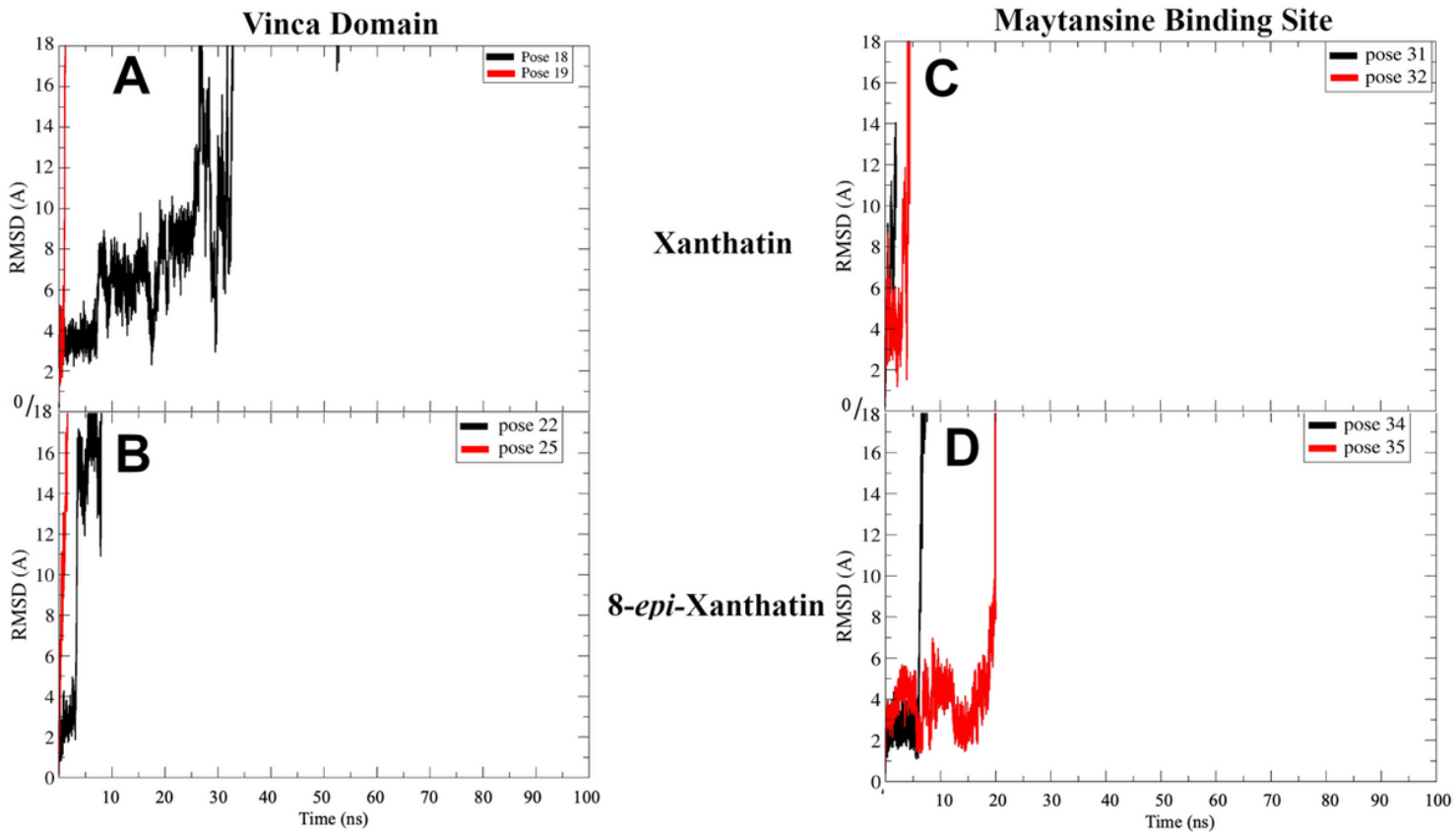
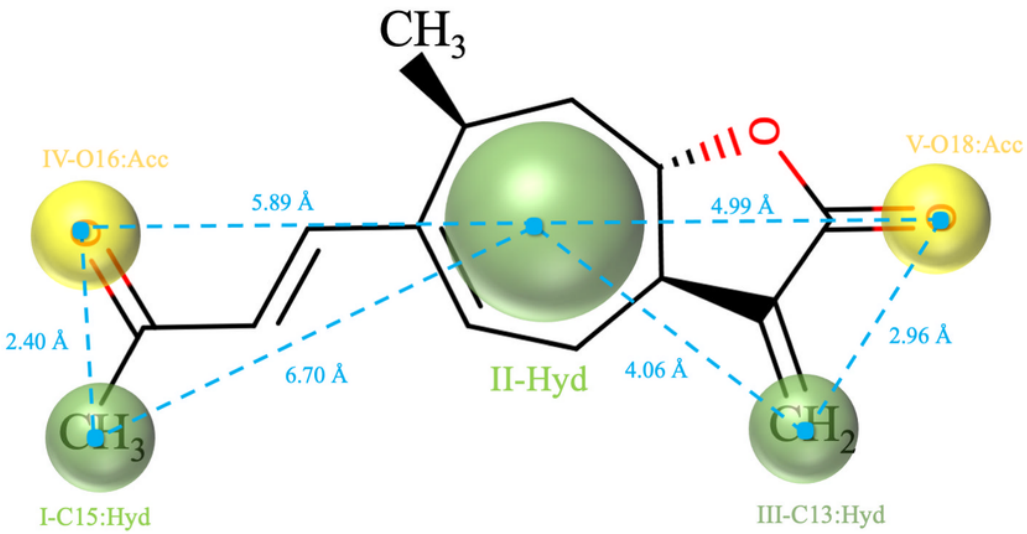


Figure 4

Root means square deviations (RMSD) corresponding to xanthanolides-vinca domain and maytansine binding site complexes. A) xanthatin-vinca domain, B) 8-epi-xanthatin-vinca domain, C) xanthatin-maytansine binding site, D) 8-epi-xanthatin-maytansine binding site



Pharmacophoric points distance proposed by Wang and coworkers	
I-II	4-9 Å
II-III	4-8 Å
III-IV	3-5 Å
V-II	4.5-7 Å
II-IV	4.5-7 Å
IV-I	5-6 Å

Figure 5

Pharmacophoric points proposed for xanthanolides compared with the pharmacophore model suggested by Wang Y. and coworkers in 2016 *[54]*. The green and yellow spheres represent the hydrophobics (Hyd) and acceptor (Acc) pharmacophoric points proposed for xanthanolides

Supplementary Files

This is a list of supplementary files associated with this preprint. Click to download.

- SupplementaryMaterials.docx